

Tape casting of bronze-graphite sheets for tribological applications

J.-E. Bidaux¹, V. Sonney¹, H. Hamdan¹, E. Carreño-Morelli¹, C. Bonjour², P. Bosc³

¹Design & Materials Unit, University of Applied Sciences Western Switzerland, CH-1950 Sion, Switzerland

²ChirMat Sàrl, CH-1870 Monthey, Switzerland

³Kugler Bimetal SA, CH-1219 Le Lignon, Switzerland

Abstract

The fabrication of bronze and bronze-graphite sheets by tape casting has been investigated. Slurries composed of powder, solvent, plasticizer and binder have been used. Green tapes have been produced, debinded and sintered. Pressureless sintering and hot pressing have been used for consolidation. The density of the sintered sheets depends on the sintering method and on the presence of graphite. Optical and scanning electron microscopy observations show a uniform dispersion of the graphite lubricant. The sheets are malleable. Pin-on disc tests show improved tribological properties.

1. Introduction

Tape casting is a cost effective technique to fabricate ceramic and metallic sheets from powders. A low viscosity slurry consisting of powder, solvent and binder is spread on a flexible moving plastic sheet [1-5]. After solvent evaporation, the green sheet is consolidated by debinding and sintering. As shown in a previous work, tape casting can be a suitable technique for manufacturing low friction coatings for steels [6]. Particularly attractive is the possibility to produce multilayered coatings or gradient structures by alternating sheets with different compositions. However, a condition for the successful implementation of these developments is the ability to produce sheets with reliable properties. In the present work, the focus is placed on the manufacturing of free-standing homogeneous and malleable bronze sheets with well dispersed solid lubricant to enhance the tribological properties. The effects of the applied pressure during sintering on the final microstructure, porosity and tribological properties are investigated.

2. Experimental

Slurries were prepared using the following constituents:

- 1) Cu-8wt%Sn-1wt%Ni (CuSnNi) prealloyed, gas atomised powder, $D_{v10}=15.7\mu\text{m}$, $D_{v50}=30.7\mu\text{m}$, $D_{v90}=52.7\mu\text{m}$ (Fig. 1a)
- 2) Synthetic graphite powder, $D_{v10}=7.4\mu\text{m}$, $D_{v50}=28.1\mu\text{m}$, $D_{v90}=75.1\mu\text{m}$ (Fig. 1b)
- 3) Methyl Ethyl Ketone (MEK) solvent, purity $\geq 99\%$
- 4) Ethyl Methacrylate Copolymer (EMC) B-72 binder
- 5) Dibutyl Phthalate (DBP) plasticizer, purity $\geq 99\%$

The formulations used in this work are shown in Tables 1 and 2. The constituents were poured into a polypropylene jar with steel balls. Wet ball mixing was carried out during 4h. Green tapes were fabricated using a custom made tape-casting device (Fig. 2). A silicone-coated Mylar foil was used as a carrier surface. The tape thickness was controlled using a micro-adjustable doctor blade. The tapes were then dried until complete evaporation of solvents. This could take 5 min to 6 h depending on the thickness of the sheet. After drying, the tapes were peeled off from the carrier surface and cut to the desired shape. Dried tapes, 10 cm wide, with thicknesses ranging from 0.2 mm to 1.5 mm were obtained.

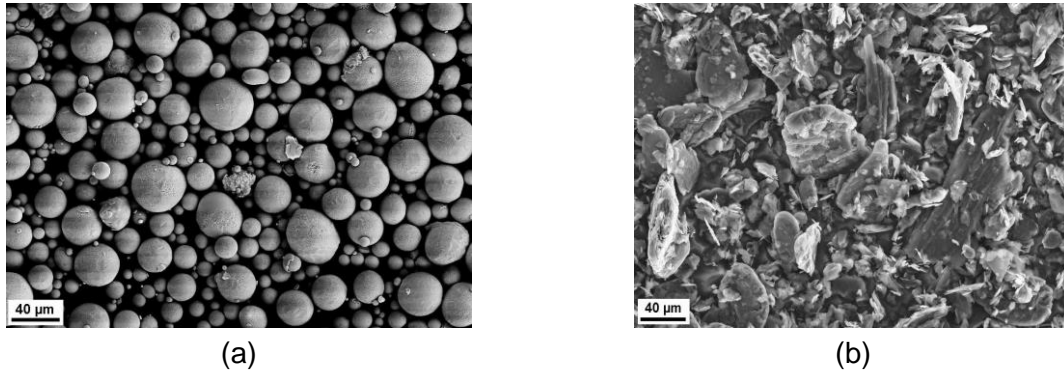


Figure 1: SEM observation of CuSnNi powder (a) and graphite powder (b)

Table 1:
CuSnNi slurry composition

Component	Weight percent [%]
CuSnNi powder	88.0
MEK solvent	7.0
EMC binder	4.0
DBP plasticizer	1.0

Table 2:
CuSnNi-graphite slurry composition

Component	Weight percent [%]
CuSnNi powder + 2wt% graphite	89.6
MEK solvent	7.0
EMC binder	2.6
DBP plasticizer	0.8

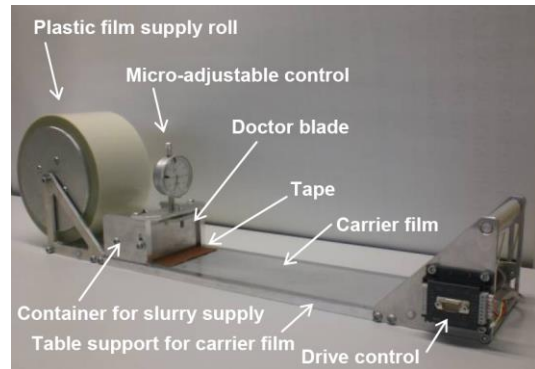
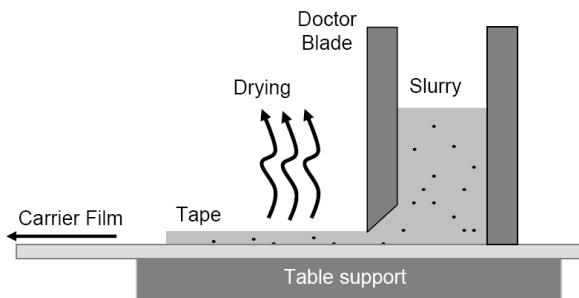


Fig. 2 Principle of tape casting (a) and experimental set-up (b)

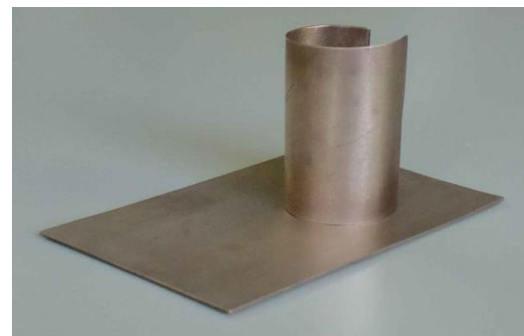
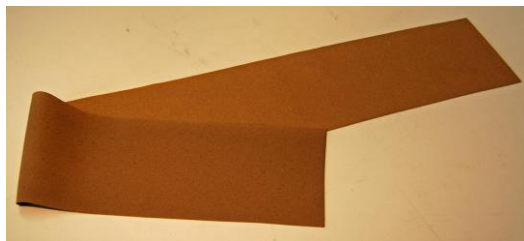


Fig. 3 Tape cast CuSnNi-2wt% graphite: green sheet (a), as sintered and bended sheets showing good malleability (b)

Two different sintering conditions were used and compared: pressureless sintering and hot pressing.

Pressureless sintering: Green tapes were debinded and sintered without pressure (other than atmospheric pressure), in a conventional SOLO 111 furnace under cracked ammonia atmosphere (75% H₂ and 25% N₂). The green tapes were placed into the oven on an Al₂O₃ substrate. The temperature was first increased at 7°C/min up to 450°C. A 30 min hold time was used at 450°C to complete binder and additives removal. The tapes were sintered at 850°C during 60 min. As shown in Fig. 3 b the resulting sintered sheets are malleable. They can be bent without cracking. Detailed mechanical characterisation is in progress.

Hot-pressing: Green tapes were sintered in a SINTRIS 10 ST/V hot press according to the following procedure. Green discs, 30 mm in diameter, stamped from the tapes, were stacked on a double action graphite tooling consisting of a die and two cylindrical pistons previously coated with boron nitride. First compaction was done at 400°C for 1 min under 50 MPa, to burn off both binder and additives. Then, also at 50 MPa, hot compaction was performed at 780°C for 15 min. The whole process was done under argon atmosphere. Sintered discs of different thicknesses were obtained by varying the number of layers. Using this method sintered compacts with densities about 97-99% of theoretical density could be produced.

Friction and wear tests were performed with a CSEM tribometer pin-on-disc machine with ball on disc contact. A 100Cr6 steel ball (6 mm diameter) was chosen as the contact tip. Dry tests were conducted at room temperature, under normal load of 5 N, at constant sliding speed of 0.1 m/s, on a total sliding distance of 1300m. During testing, the coefficient of friction was monitored as a function of the sliding distance. Wear of the contact surface was evaluated after test by mass loss measurements.

Particle size distribution was measured with a Malvern Mastersizer 2000 laser diffractometer. Powder morphology and microstructure of the green and sintered sheets were investigated by scanning electron microscopy using a LEO 1525 microscope. Density measurements were performed by the Archimedes method. Thermogravimetric analysis was performed using a Setaram TAG 24 device to estimate the debinding temperatures. Metallographic observations of the sintered bodies were performed using an Olympus AX70 optical microscope.

3. Results and discussion

Microstructure

Fig. 4 and 5 show the microstructure of the sintered sheets. The sheets sintered under applied pressure (hot pressed) are almost fully dense. As shown in Table 3 densities of 99 % and 97 % relative to the theoretical density are measured in the case of CuSnNi and CuSnNi-2wt% graphite respectively. Graphite is well distributed in the matrix. Unexpected was the high density, 97%, of the pressureless sintered CuSnNi sheet. This strong densification might be the result of the relatively small size, high sphericity and high purity of the CuSnNi powder. A significantly lower density, 77%, is measured for CuSnNi sheets with 2wt% graphite. The presence of graphite clearly prevents sintering and densification of the CuSnNi particles. In this case, porosity is certainly open.

Additional observations were performed by scanning electron microscopy (Fig. 6). The presence of graphite in the dark areas can be seen. Porosity is mainly observed close to the graphite inclusions. Additional EDX analysis indicates a homogeneous distribution of Cu, Sn and Ni in the bronze matrix (solid solution) as expected from the phase diagram.

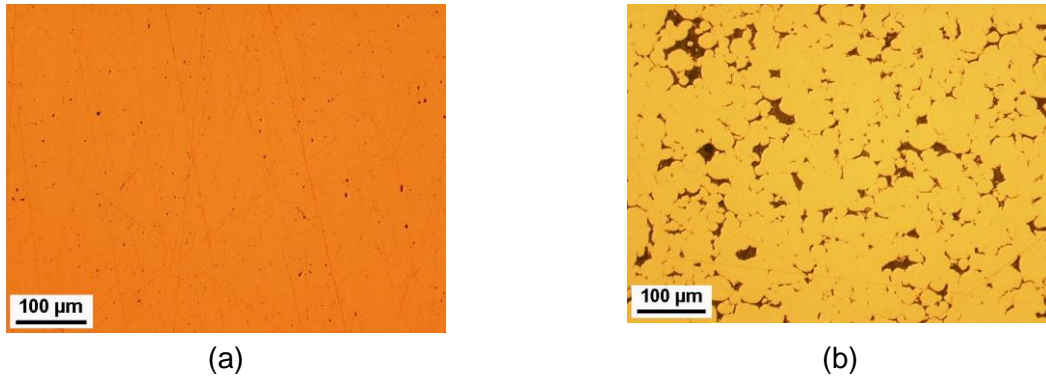


Fig. 4 Optical microscopy observations of hot pressed sheets: CuSnNi (a), CuSnNi-2wt% graphite (b)

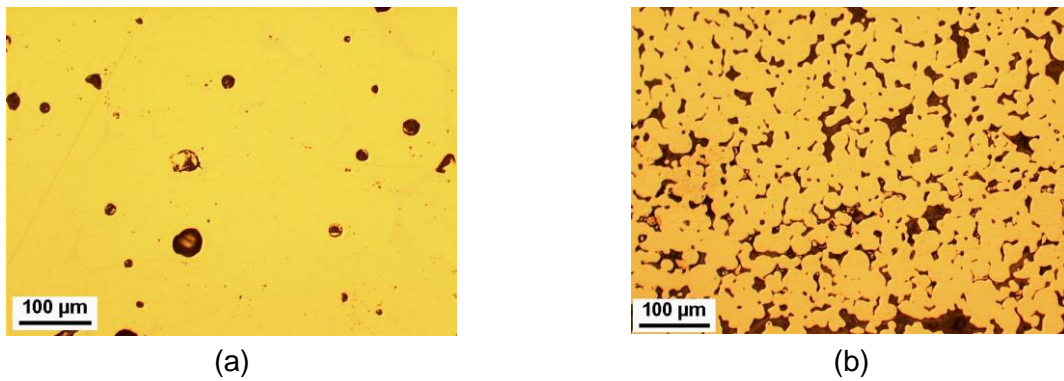


Fig. 5 Optical microscopy observations of pressureless sintered sheets: CuSnNi (a), and CuSnNi-2wt% graphite (b)

Table 3 Measured sintered sheet densities

Materials	Sintering	Density	
		g/cm ³	% *
CuSnNi	Hot pressed	8.68	99
	Pressureless	8.51	97
CuSnNi-2wt% graphite	Hot pressed	8.02	97
	Pressureless	6.43	77

* Based on theoretical densities: CuSnNi 8.77g/cm³ [7-8], graphite 2.26 g/cm³

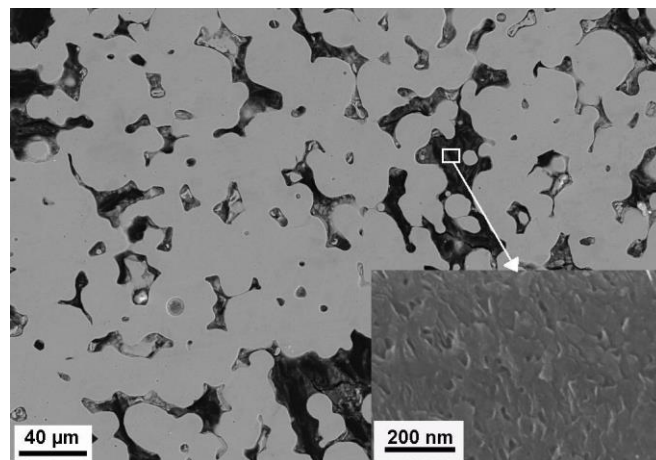


Fig. 6 SEM micrograph of a cross-section of a pressureless sintered CuSnNi-2wt% graphite sheet with a detail showing the presence of graphite in the dark areas

Tribological properties

Pin-on disc measurements of the coefficient of friction show the effect of graphite as lubricant (Fig. 7). The coefficient of friction is close to 0.8 for the sheet without graphite. The lowest coefficient of friction, close to 0.1, is measured for the hot pressed sheet with graphite. For the pressureless sintered sheet with graphite, the improvement is smaller but still significant. The improvements in the wear characteristics are in line with those of friction (Fig. 8). The best wear resistance is observed for the hot pressed material with graphite. The pressureless sintered material also exhibits a large improvement in wear resistance.

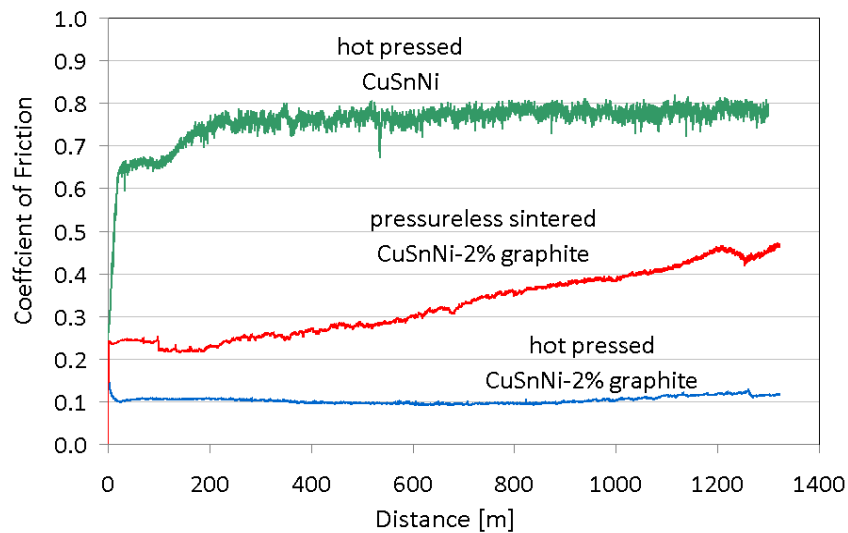


Fig. 7 Coefficient of friction as a function of sliding distance for tape cast CuSnNi and CuSnNi-2wt% graphite sheets sintered under various conditions

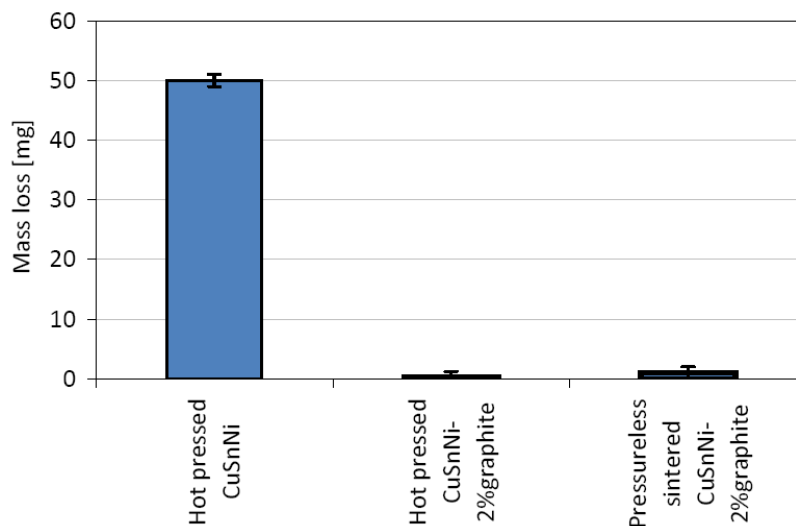


Fig. 8 Wear of tape cast CuSnNi and CuSnNi-2wt% graphite sheets sintered under various conditions; sliding distance 1300 m

Clearly, the best tribological properties are achieved by hot pressing. Nevertheless, pressureless sintering remains attractive for coatings applications. For complex geometries, it is certainly easier to implement compared to hot pressing. This, together with the good tribological properties, encourages further investigation. Another advantage, particularly in wet friction conditions, is the reservoir for liquid lubricant than can provide the pressureless sintered porous material. Tests are in progress to check whether sufficient adhesion with the substrate can be achieved.

4. Conclusions

CuSnNi and CuSnNi-2wt% graphite sheets have been produced by tape casting. The distribution of graphite lubricant is uniform. The sheets are malleable. Sintered sheets with improved tribological properties are obtained both by pressureless sintering and hot pressing. The best tribological properties are obtained for the hot pressed sheets. However, pressureless sintering provides an interesting combination of good tribological properties and easy manufacturing. These results are promising for further applications to low friction coatings for steels.

Acknowledgments

This work was supported by the Swiss Commission for Technology and Innovation CTI under Grant 9818.2 PFIW-IW. The authors thank Timcal Graphite and Carbon, Bodio, Switzerland, for kindly providing the graphite powder used in this work.

References

- [1] R. E. Mistler, V. K. Sikka, C. R. Scorey, J. E. McKernan, M. R. Hajaligol, Tape casting as a fabrication process for iron aluminide (FeAl) thin sheets, *Materials Science and Engineering*, A258 (1998) pp. 258-265
- [2] Z. S. Rak, J. Walter, Porous titanium foil by tape casting technique, *J. of Materials Processing Technology*, 175 (2006) pp.358-363
- [3] G. Stiebritz, H. Uhlenhut, M. Svec, Tape cast tungsten alloy sheet and foil, *Proc. of Euro PM2008*, European Powder Metallurgy Association, Mannheim, Germany (2008) pp.9-14
- [4] A. H. Persson, K. Broderson, A. K. Srivastava, T. Stegk, P. Blennow, S. Ramousse, Fabrication and Characterization of porous structures produced by tape casting, *Proc. of Euro PM2009*, European Powder Metallurgy Conference, Copenhagen, Denmark, 2009, vol.2, pp. 311-316
- [5] J.-E. Bidaux, H. Girard, V. Sonney, H. Hamdan, S. Rey-Mermet, E. Carreño-Morelli,, Tape casting of copper based shape-memory alloys, *Proc. of Euro PM2009*, European Powder Metallurgy Conference, Copenhagen, Denmark, 2009, vol.1, pp. 371-376
- [6] M. Cans, H. Hamdan, Y. Öner, J.-E. Bidaux, E. Carreño-Morelli, Tape casting of copper alloys for tribological applications, *Proc. of Euro PM2008*, European Powder Metallurgy Conference, Mannheim, Germany, 2008, vol.1, pp. 27-32
- [7] A. Cheng, D. Apelian, A. Lawley, W. E. Smith, P. W. Taubenblat, Effect of Nickel Additions on the Properties and Performance of PM Bearings, *Powder Metallurgy International*, Vol. 15, No4, 1983, pp. 178-182
- [8] Copper and copper alloys, *ASM Specialty Handbook*, Edited by J. R. Davis, Davis Associates, ASM International, 2001, p.547